

Hydroacoustic analysis of spatial and temporal variability of bottom sediment characteristics in Lake Kinneret in relation to water level fluctuation

Ilia Ostrovsky · Jarosław Tęgowski

Received: 13 January 2009 / Accepted: 24 November 2009 / Published online: 11 December 2009
© Springer-Verlag 2009

Abstract Rapid alterations of aquatic ecosystems associated with changing climate and growing anthropogenic stress require the development of effective and low-cost acoustic methods of bottom sediment characterization and mapping. Acoustic reflectance and scattering properties of surface bottom sediment (SBS) were characterized by energetic, statistical, spectral, wavelet, and fractal parameters of single-beam echo envelopes. A common feature of the chosen parameters is indication of energy distribution in the frequency domain and fractal description of the echo-envelope shape. Data collected with a 120-kHz single-beam echosounder along 14 regular transects were used to determine the acoustical properties of SBS, and study their spatial and temporal changes in Lake Kinneret, and their relation to sedimentological characteristics of the bottom. Special post-processing procedures were applied to remove the instability of the acoustical signal (caused by angular movement of the transducer), and the impact of the bottom slope. The influence of changing depth on the shape of the echo signal was corrected by the depth normalization procedure. Sediment grain size in the upper few-centimeter layer was studied based on grab samples. Some acoustical parameters showed close association with granulometric variables and organic matter content in the upper sediments. The observed effect of water level fluctuation on several

echo parameters was apparently associated with changes in gas content in the SBS. Spatial distributions of some echo parameters were very stable with time; other parameters showed large changes in the central part of the lake, but were nearly unchanged at the lake periphery. Overall, the suggested approach is a useful tool for investigation of fine modifications of SBS properties in aquatic ecosystems.

Introduction

The surface bottom sediment (SBS) is a functionally important element of aquatic ecosystems. In shallow aquatic systems such as estuaries, coastal waters, lakes, and reservoirs, intensive material exchange between the bottom and the water may determine nutrient fluxes and the productivity of the entire ecosystem (Jickells 1998; Mann 2000; Middelburg and Levin 2009). The SBS holds significant information about settling materials and biogeochemical processes at the bottom (Meyers and Teranes 2001). Rapid alterations of aquatic ecosystems associated with changing climate and increasing anthropogenic stress require fast, effective, and low-cost monitoring of the SBS, and an understanding of the processes affecting its transformation. Methods of bottom sediment characterization are, therefore, expedient in aquatic ecology, geology, habitat mapping, ecosystem management, and modeling (Godet et al. 2009).

Measuring specific parameters of bottom sediments using traditional sampling procedures (dredging, coring, etc.) requires immense efforts when large bottom areas should be investigated, especially when sedimentary parameters are spatially heterogeneous and temporally variable. In contrast to conventional sediment sampling, hydroacoustic technology allows rapid scanning over large

I. Ostrovsky (✉)
Israel Oceanographic & Limnological Research,
Yigal Allon Kinneret Limnological Laboratory,
P.O. Box 447, Migdal 14950, Israel
e-mail: ostrovsky@ocean.org.il

J. Tęgowski
Institute of Oceanography, University of Gdańsk,
al. Marszałka Piłsudskiego 46,
81-378 Gdynia, Poland

areas of bottom sediments synoptically to specify and map sedimentary parameters (Tęgowski 2005; Wienberg and Bartholomä 2005; van Walree et al. 2005). As a result, acoustic seabed classification is an area of extensive development. This methodology is widely used as a fast and efficient tool for bottom type recognition and classification of benthic habitats in marine, brackish water, and freshwater environments (e.g., Tęgowski 2006; Anderson et al. 2007, 2008; Mortensen et al. 2009). The existing acoustic methods of surface sediment characterization have, however, specific obstacles associated with the rather complicated inverse theory of scattering of acoustical signal on rough and layered sediments (Tęgowski et al. 2006). Some echo-envelope parameters or their combinations allow distinguishing between different types of bottom, such as rocky and stony bottom from sandy and muddy sediments. For example, commercially used RoxAnn or QTC systems allow bottom classification with high efficiency (Hamilton et al. 1999). The RoxAnn system uses a small quantity of echo-envelope parameters (energies of first and second echoes), whereas the QTC uses as much as 166 parameters, but these parameters are unknown for users. Characterization of the “same” type of bottom sediments is still challenging. The criteria of bottom classification or characterization established in one case seldom apply to other cases, and “a site-specific approach”, which includes comparison of physical and acoustic properties of sediments at specific locations, is required. The problem with the translation/interpretation of echo-envelope parameters in terms of seafloor morphological features is exacerbated by the fact that sediments having similar granulometric composition may considerably differ in physicochemical properties. These properties depend on the geological and sedimentological background of the investigated area, the particulate composition of the sediment, gas bubble content (Wilkins and Richardson 1998), and abundance of benthos (Holliday et al. 2004), which directly influence the shape and energetic characteristics of the scattered acoustical signal. Consequently, it is necessary to find specific acoustical variables that correspond to defined seafloor characteristics.

In this paper we used data collected with a high-frequency single-beam echosounder during several acoustic surveys on Lake Kinneret (Israel) to test a set of different energetic, statistical, spectral, and geometrical parameters that describe the bottom echo signal, to characterize the bottom sediments based on data collected during six hydroacoustic surveys. The key test was performed along an offshore standard transect, where the changes in bottom sediments have been intensively investigated during several sampling campaigns. Then, we mapped the distribution of the parameters in the whole lake, and analyzed their consistency and inter-seasonal variability. The measure-

ments of method-defined parameters enhance the probability of finding the distinctive echo-envelope features associated with specific sediment parameters in the investigated area.

Information about energy distribution in the frequency domain, and analysis of echo-envelope shape have been used to specify the types of bottom or recognize the bottom habitats (e.g., Anderson et al. 2007). In this study we related some features of bottom echo envelopes directly with physical and chemical properties of sediments, and examined the spatial and temporal variations of sedimentary parameters in relation to water level fluctuations in a medium-size lake. The presented method may be a powerful tool for monitoring of bottom sediments, and for investigation of their alterations associated with rapid modern changes in aquatic ecosystems.

The lake

Lake Kinneret (the Sea of Galilee) is located at about -210 masl (meter above sea level) in the northern part of Israel (Fig. 1). The lake is monomictic and warm, with a surface area of 168 km^2 . Its average and maximum depths are 22 m and 42 m, respectively. The Jordan River is the major inflow, and water pumped into the National Water Carrier constitutes the main outflow. Due to annual and multi-annual asymmetry in the water inflow and outflow, the water level is variable (1.5–2.0 m on an annual basis, and 4–6 m on a multi-annual basis). During the peak of inflows to the lake (winter–spring), the allochthonous load does not exceed (by mass) 14% of the particles found in the



Fig. 1 Map showing the location of Lake Kinneret (Israel), its bathymetric map at water level of -209 masl, and standard transects of acoustic surveys

lake water column (Parparov and Yacobi, unpublished data). The sedimentary record of the last ca. 3,000 years indicates that primary production in this mesotrophic lake has varied in the past over a range similar to that observed presently (Dubowski et al. 2003). Bottom sediments are usually sandy in the shallower zone, and muddy in the pelagic zone (Ostrovsky and Yacobi 1999). The sediments in the northern and western parts of the lake are richer in fine detrital material, while in the central and eastern areas calcium carbonate is relatively an important component (Singer et al. 1972; Serruya et al. 1974).

Materials and methods

Acoustic sampling

Acoustic properties of bottom sediments were studied based on data collected with a downward-oriented Biosonics DE5000 narrow-beam echosounder (6.5°) operating at 120 kHz. The pulse width was set to 0.2 ms, with a sampling rate of five pings s⁻¹. The lower threshold for data collection was set to -75 dB or -80 dB. Acoustic data were collected along 14 standard acoustic transects, the locations of which have been specified elsewhere (Ostrovsky and Walline 2001). Twelve transects were positioned perpendicular to the lake shoreline, while two were located in the central northern and southern areas. These transects cross areas with all types of bottom sediments.

Signal processing and bottom echo parameters

For our computation, only the data collected at a boat speed range of four to five knots were used, to avoid the effect of changing inclination of the echosounder transducer on the acoustic return from the bottom (e.g., von Szalay and McConnaughey 2002). The backscattered signal was corrected regarding geometrical spreading of the acoustical wave and sound attenuation in the water body. We used the time varied gain (TVG) function 30log₁₀(R), where R is the distance from the echosounder transducer to the bottom.

Another necessary correction of the echo envelope was compensation of dependency of the echo length on depth, which is the result of the increase in footprint diameter in proportion to the water depth, whereby the backscatter area and echo duration increase as well. A linear dependency of echo length on depth was applied (Caughy and Kirlin 1996). For the chosen reference depth H₀, the reference time t' was calculated. Then, the time in echo pulse should be rescaled as follows:

$$t' = t \cdot \frac{H_0}{R} \tag{1}$$

The proposed correction is equivalent to the change of sampling frequency established by the reference time t' and mean echo compression for R>H₀, and echo elongation for the reverse case. In our computations, the reference depth H₀ was 10 m. The choice of the 30log₁₀(R) TVG function corresponds to compensation of total loss of intensity due to depth increase (Pouliquen 2004). The next procedure eliminated echo signals with energy lower than 75% of energy of all the 20 echoes in the chosen, consecutive windows. This algorithm distinguished echoes of the most perpendicular acoustical beams to the bottom surface, and eliminated echoes registered from inclined echosounder transducer position.

The selection of echo parameters expected to be sensitive to different seabed morphological features was done based on published results (e.g., Pace and Ceen 1982; van Walree et al. 2005), and our own experience (Tęgowski 2006). The echo-envelope parameters used (namely, energetic, spectral, statistical, wavelet, and fractal) are mainly indicators of energy distribution in the frequency domain, and fractal description of the echo-envelope shape.

Energetic and statistical features are an important group of echo parameters used in acoustical classification of bottom sediments (Tęgowski and Łubniewski 2002; Tęgowski et al. 2003). For echo envelope x(t) with duration T₀, the total intensity I(t) is proportional to the square of the echo pressure. The echo pulse energy is defined as:

$$E = \int_0^{T_0} I(t)dt \tag{2}$$

The significant parameter that describes the acoustical energy scattered at the bottom surface is the energy of the first part of the echo (E_s, from the beginning to its maximum value), while information about the energy of the volume scattering in the sediment (E_v) is contained in the echo tail (Sternlicht and de Moustier 2003). The ratio of both energies (E_s/E_v) can be an indicator of seafloor acoustic hardness.

The bases of spectral parameters are echo-envelope spectral moments of the rth order:

$$m_r = \int_0^\infty \omega^r S(\omega)d\omega \tag{3}$$

where S(ω) is the Fourier power spectral density, and the moment order is r=0, 1, ... , 7.

The combination of spectral moments are spectral widths ε², ν², and spectral skewness γ defined in Clough and Penzien (1975):

$$\varepsilon^2 = \frac{m_0 m_4 - m_2^2}{m_0 m_4}$$

$$v^2 = \frac{m_0 m_2}{m_1^2} - 1$$

$$\gamma = \frac{\tilde{m}_3}{\tilde{m}_2^{3/2}}$$

These parameters were used for the acoustical signal characterization (Tęgowski et al. 2003; Tęgowski 2006). The slope β of the power spectral density function is the basis of a specific form of fractal dimension (D_{FFT}) estimation. Mandelbrot (1982) proved that $D_{\text{FFT}} = (5 - \beta)/2$.

A group of very sensitive parameters for echo signal changeability includes the coefficients of wavelet transformation, and respective wavelet energies (Atallah et al. 2002). For each analyzed echo envelope, the wavelet energy content was computed using the 7-channel dyadic decomposition (scale $a=2^j$, $j=1, \dots, 7$) with Coiflets, Daubechies, and Meyer wavelets.

Moreover, the wavelet transformation coefficients were the source of Hurst exponent determination of the echo envelope (and subsequently the Hausdorff dimension $D_{\text{H,Daub7}} = 2 - H$) via the averaged wavelet coefficient method (Simonsen et al. 1998; Tęgowski 2005).

The kriging interpolation technique was used for mapping the spatial distribution of echo parameters of soft sediments. This method proves to be efficient for reproducing the heterogeneous distribution of different environmental variables (e.g., Oliver and Webster 1990).

All calculated parameters were used for seafloor classification. Two classes of segmentation procedures were applied: (1) the fuzzy c-means (FCM) data clustering method (Bezdeck et al. 1984), and (2) the self-organized Kohonen's neural network (Kohonen 1987). A principal component analysis (PCA) was applied to the 62 parameters defined above. The product of PCA are principal components (variation >98%), which were the input to segmentation procedures. The choice of fuzzy logic in clustering algorithm was justified by the complexity of the physical phenomenon of sound scattering at the bottom, and the level of inevitable echo signal disturbances introduced by environmental conditions.

Groundtruth data

Bottom sediment samples were collected at several stations located along a northwestern offshore transect on the northwestern side of the lake, where all types of soft sediments were present. Sediment sampling was carried out with an Ekman-Birge grab during different seasons, starting in 1993. In order to avoid large losses of upper sediments due to overfilling of the grab, the samples used for analysis were collected only when the sediment level in the sampler

compartment was at least 5 cm below the upper flaps. Although material collected with the grab could lose a couple of millimeters of the organic-rich fluffy layer at deep locations (Ostrovsky 2000), this way of sampling provided seasonally unvarying data about lateral changes in sedimentary parameters (see below), which is suitable for groundtruth information for bottom characterization.

It is important to stress that using the grab sampling for groundtruthing acoustic measurements was possible because the depth of sound penetration into the bottom (usually <50 cm for most types of soft sediments in Lake Kinneret) was comparable with the thickness of sediments collected with the Ekman-Birge grab. The thickness of the layer that contributes to the volume scattering of the penetrating pulse is associated with attenuation of the compressional wave in the sediment. The latter parameter typically varies from 0.1 dB/ λ for unconsolidated muddy sediments, to 1 dB/ λ for sandy sediments (Hamilton 1972; Bowles 1997), where $\lambda = 1.25$ cm is the wave length at given sonar frequency and sound speed in water ($\sim 1,500$ m s⁻¹). Furthermore, the presence of high amounts of gas bubbles in surface sediments (see below) may significantly increase the sound attenuation, and also form a scattering screen for the high-frequency acoustical pulse (Robb et al. 2006). Hence, the bottom samples collected with the Ekman-Birge grab could adequately characterize the sediment layer penetrated by sounding pulses.

Grain size composition in collected sediment samples was estimated using a standard hydrometric method (Buchanan and Kain 1971). Further processing of the particulate matter was as specified by Ostrovsky (2000). In brief, determination of organic matter content (OMC) in the sediments was performed on subsamples treated immediately. The dry weight of subsamples was estimated by drying at 80°C for 24 h. Loss on ignition, equivalent to OMC, was measured after combustion of pre-dried material in a muffle furnace at 550°C for 4 h.

To associate the data collected at different water levels to the same bottom location and sediment type along the transect, all data were plotted relative to a "reference depth", which denotes the location depth at the highest water level of -209 masl.

Results

The general pattern of soft sediment distribution was studied along the northwestern offshore transect, which spanned between the northwest part of the lake and its center. The bottom depth-specific slopes along this transect are close to those in the entire lake. In the shallowest part of this transect, the sand fraction was the most abundant (>80% of dry weight) down to 8 m depth. Sand was

virtually absent at depths >17 m (Fig. 2a). Despite that shells of mollusks may be an important component of the soft bottom sediments elsewhere, they were virtually absent in our samples. This is related with the fact that in Lake Kinneret snails and bivalves inhabit only the shallow littoral zone (<5–8 m depth; Ostrovsky et al. 1993), which was excluded from our acoustic sampling.

The OMC, expressed as the proportion of organic material per dry weight of sediment, showed a gradual increase from the shallowest location to a depth of 16–20 m, and then was nearly unchanged to the lake center (Fig. 2b). The data also show low variability of this variable with time. It is notable that the lateral variations of OMC and water content in the upper 2–4 mm sedimentary layer collected by SCUBA (Ostrovsky and Yacobi 1999) gradually increased from the shallowest areas toward the lake center, suggesting greater “softness” of surface sediments and possibly higher rates of net accumulation at the lake center.

The changes in some acoustical characteristics measured during different sampling campaigns along the northwestern offshore transect show clear depth-dependant patterns (Fig. 3), which apparently reflect the gradual changes in sedimentary properties. For instance, the change in the $\log(E_s/E_v)$ ratio displays a decrease with bottom depth, while the fractal dimension (D_{FFT}) and $\log(\nu^2)$ showed gradual increases with depth along the transect. In order to specify which acoustic parameters may better portray the sediment properties, correlation coefficients between echo-envelope and sedimentary parameters were computed.

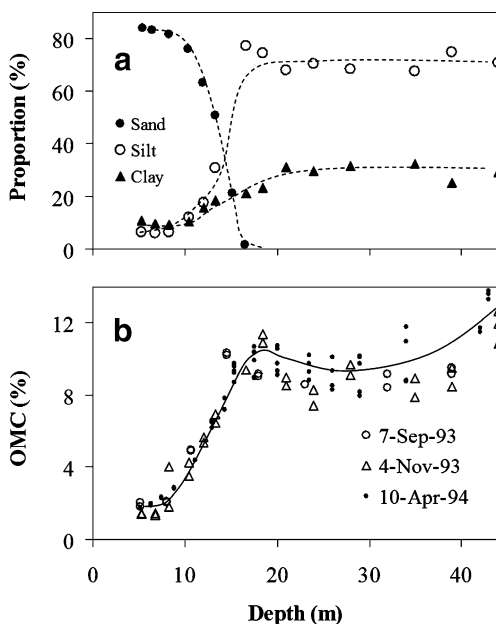


Fig. 2 Characteristics of bottom sediments along the northwestern offshore transect: **a** proportion of sand, silt, and clay; **b** organic matter content (OMC). Data were collected during three surveys in 1993 and 1994 with an Ekman-Birge grab. Each point represents the average of two subsamples

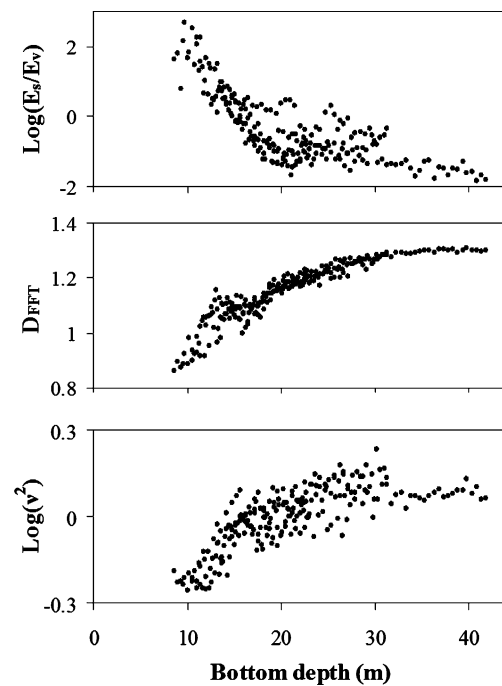


Fig. 3 Changes in selected echo parameters along the northwestern offshore transect (see “Materials and methods” for parameter explanations). Data were collected during six acoustic surveys from 2002 to 2007. The data were binned using a 0.5-m depth interval, and each point represents the mean of usually 10–100 measurements

Taking into account the possible effect of water level on certain properties of soft sediments (see below), the calculations were based on acoustic measurements performed in November 2003, when water level in the lake was identical to that during the time of grab sampling. The results presented in Fig. 4 show that some echo parameters are well correlated with sedimentological variables. For instance, $\log(M_2)$ was positively correlated with OMC, and negatively correlated with the proportion of sand.

Our acoustic sampling of the bottom covered a period of large changes in water level. Extremely low water level (–214.4 masl) took place in autumn 2002; then, after a vast flood during winter–spring in 2002–2003, it reached its possible maximum (–209.0 masl). Measurements carried out at two central transects, along which bottom depth and sediment type were nearly unchanged, revealed a high correlation ($r > 0.9$) between water level and some echo parameters, e.g., the spectral width – $\log(\epsilon^2)$ and $\log(E_s/E_v)$ ratio. An example of such a relationship between $\log(\epsilon^2)$ and water level is shown in Fig. 5.

The survey-specific maps of two echo parameters at different dates are shown on Fig. 6. The spatial distributions of D_{FFT} at low water level in 2002 (Fig. 6a) and at high water level (Fig. 6b) were very close, and had the highest values in the central part of the lake. In contrast, the spatial distribution of $\log(E_s/E_v)$ ratios in 2002 (Fig. 6c) and 2003 (Fig. 6d) were different in the central part of the lake, while

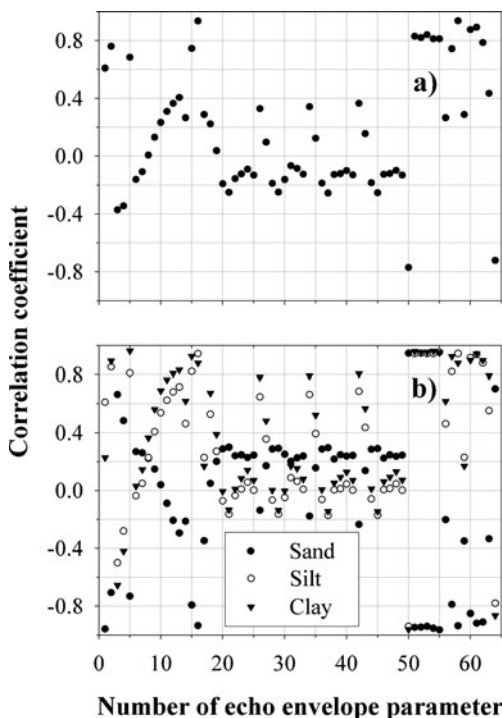


Fig. 4 Correlation coefficients between echo-envelope parameters and parameters of the upper layer of bottom sediments: **a** organic matter content, **b** percentage of sand, silt, and clay. The echo-envelope parameters are presented as numbers on the x-axis, as follows. 1, $\log(E_0)$; 2, $\log(E_v)$; 3, $\log(E_2)$; 4, $\log(E_s)$ (E_0 is the echo energy of signal scattered in a thin layer overlaying the bottom, E_2 the energy of the second echo); 5, D_{FFT} (fractal dimension computed with the FFT method); 6, $\log(m_0)$; 7, $\log(m_1)$; 8, $\log(m_2)$; 9, $\log(m_3)$; 10, $\log(m_4)$; 11, $\log(m_5)$; 12, $\log(m_6)$; 13, $\log(m_7)$; 14, $\log(M_0)$; 15, $\log(M_1)$; 16, $\log(M_2)$; 17, $\log(M_3)$ (M_r are statistical central moments of the r th order); 18, $\log(Edb_{3,1})$; 19, $\log(Edb_{3,2})$; 20, $\log(Edb_{3,3})$; 21, $\log(Edb_{3,4})$; 22, $\log(Edb_{3,5})$; 23, $\log(Edb_{3,6})$; 24, $\log(Edb_{3,7})$; 25, $\log(Edb_3)$; 26, $\log(Edb_{5,1})$; 27, $\log(Edb_{5,2})$; 28, $\log(Edb_{5,3})$; 29, $\log(Edb_{5,4})$; 30, $\log(Edb_{5,5})$; 31, $\log(Edb_{5,6})$; 32, $\log(Edb_{5,7})$; 33, $\log(Edb_5)$; 34, $\log(Edb_{7,1})$; 35, $\log(Edb_{7,2})$; 36, $\log(Edb_{7,3})$; 37, $\log(Edb_{7,4})$; 38, $\log(Edb_{7,5})$; 39, $\log(Edb_{7,6})$; 40, $\log(Edb_{7,7})$; 41, $\log(Edb_7)$; 42, $\log(Edb_{12,1})$; 43, $\log(Edb_{12,2})$; 44, $\log(Edb_{12,3})$; 45, $\log(Edb_{12,4})$; 46, $\log(Edb_{12,5})$; 47, $\log(Edb_{12,6})$; 48, $\log(Edb_{12,7})$; 49, $\log(Edb_{12})$ ($Edb_{r,j}$ is the energy of Daubechies wavelets of the r th order and scale $a=2^j$, Edb_r the sum of wavelet energies for $j=1, \dots, 7$); 50, $\log(c_r)$ (c_r is the echo envelope radius of autocorrelation); 51, $\log(D_{H,coif3})$; 52, $\log(D_{H,meyr})$; 53, $\log(D_{H,db3})$; 54, $\log(D_{H,db7})$; 55, $\log(D_{H,db12})$ (fractal dimension computed using Coiflets, Meyer, and Daubechies wavelets); 56, $\log(\omega_0)$ ($\omega_0=m_1/m_0$ is the mean frequency); 57, $\log(\nu^2)$; 58, $\log(\varepsilon^2)$; 59, $\log(\gamma)$; 60, $Edb_{5,1}/E_v$; 61, $Edb_{5,2}/E_v$; 62, Edb_5/E_v ; 63, c_r/D_{FFT} ; 64, $\log(E_s/E_v)$. Correlation coefficients were calculated for data collected at water level of about -210 masl

the lateral changes in this ratio in the littoral and sublittoral areas remained the same.

Discussion

The data presented in this paper clearly indicate regular changes of acoustical characteristics, which were coherent with the changes in sedimentary variables along offshore transects.

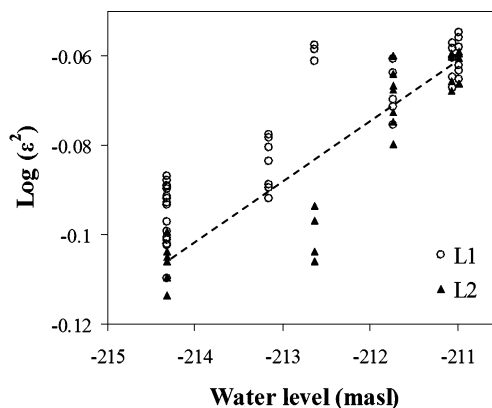


Fig. 5 Relationship between the spectral width ε^2 and water level along two central transects (L1 and L2) in Lake Kinneret. Transects L1 (the mean bottom depth is 34 m at water level of -209 masl) and L2 (the mean bottom depth is 41 m at water level of -209 masl) are positioned in the central southern and central northern parts of the lake, respectively. Other explanations are as in Fig. 3

The higher fractal dimension (D_{FFT}) values suggest the more complex shape of the irregular echo signal. The increase in D_{FFT} with depth indicates that muddy sediments in deep zones are of more complex layered structure than shallower sediments with higher proportions of sand. In other words, sediments in shallower areas should be better mixed by intensive water motions than sediments in deeper zones. This is supported by our observations on the vertical

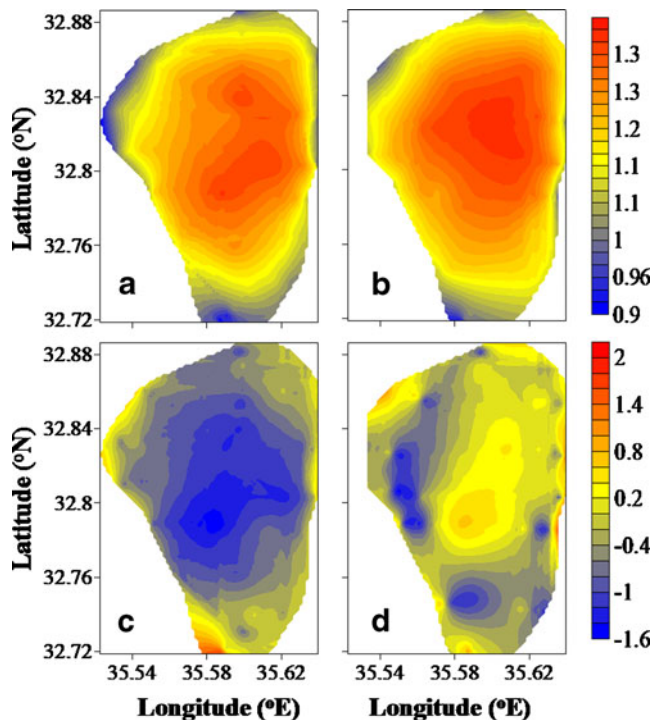


Fig. 6 Spatial variability in **a, b** D_{FFT} , and **c, d** $\log(E_s/E_v)$ in Lake Kinneret at low water level of -214.4 masl on 30 October 2002 (**a, c**), and at high water level of -211.0 masl on 19 November 2003 (**b, d**). See explanations in the text

structures of sediment cores taken in different parts of the lake (Fig. 7). Sediment cores taken in shallower areas (12 m depth), which are strongly affected by highly energetic internal waves (Ostrovsky and Yacobi 1999), are rather homogeneous vertically. In contrast, soft cohesive sediments in deep zones are periodically influenced by extreme loading of clay-rich allochthonous particles during years with intensive floods. As a result, the carbonate content in such layers sharply decreased (Dubowski et al. 2003). Moreover, the deep sediments contain horizontally elongated gas pockets (Fig. 7b) that may also affect sound propagation in sediments, and thus its acoustic parameterization. These findings confirm the hypothesis that layers of bottom sediments have a fractal structure, and can be depicted by the shape of the acoustic echo (Ishimaru 1978).

D_{FFT} spatial distributions were similar at different water levels, and displayed the highest values in the deep central part of the lake, suggesting an increase in complexity of sediment layered structure from the peripheral areas toward the lake center. The spatial distributions of $\log(E_s/E_v)$ displayed different behavior in response to the water level in the central part of the lake and in shallower areas, where it was fairly stable. Such a performance of the $\log(E_s/E_v)$ parameter may be evident, taking into account the negative correlation of this parameter with OMC (Fig. 4), and positive correlation of this parameter with water level in the deep part of the lake. The latter correlation also reflects the inverse relationship of $\log(E_s/E_v)$ with volumetric capacity of gases in sediments. This can be deduced based on the profuse methane ebullition

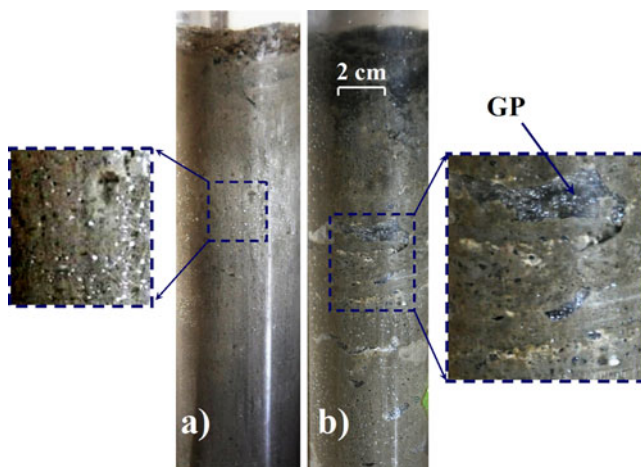


Fig. 7 Sediment cores collected in Lake Kinneret at sampling sites where water depth was **a** 12 m, and **b** 38 m. At the shallower location (**a**), the sediment core is homogeneous below the upper 1-cm fluffy layer; methane bubbles are seen in sediments below the upper 5-cm layer. At the deep location (**b**), the sediment core is laminated below the upper 3-cm fluffy layer; methane bubbles are numerous in sediments below the upper 1.5-cm layer; horizontally oriented gas pockets (GP) are seen. The pressure-corrected radii of numerous round-shaped bubbles were 0.1–0.4 mm in both cores collected on 13 October 2009 at low water level of -214.3 masl

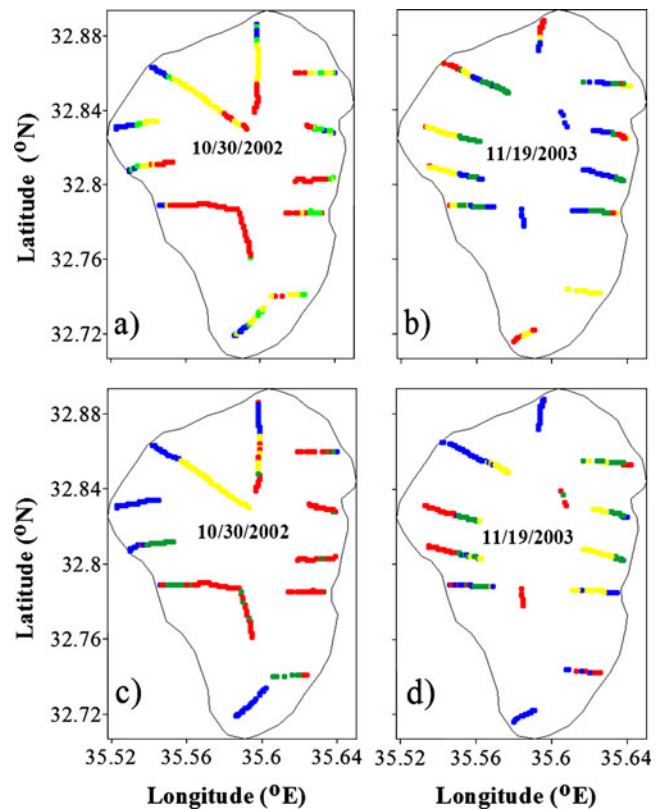


Fig. 8 Seafloor classification using two kinds of segmentation procedures: **a, b** fuzzy c-means (FCM) data clustering method; **c, d** self-organized Kohonen's neural network. The principal components were the input to the segmentation procedures. Four classes are shown by different colors. The classification shows large differences between the two sampling dates

from deep organic-rich sediments at low water levels (Ostrovsky et al. 2008). It is remarkable that in the shallower organic-poor sediments, where methane emission was not detected or negligible in different years, no effect of water level on $\log(E_s/E_v)$ took place. Thus, the correlations between certain echo parameters (ε^2 and E_s/E_v ratio) and water level were apparently associated with inter-annual changes in the amount of bubbles in the sediment due to alteration of hydrostatic pressure at the bottom (Ostrovsky 2003). Low hydrostatic pressure was responsible for large gas emission in 2001 and 2002. Still, the less intensive bubble emission rate in 2002 (compared to 2001) could be associated with the residual amount of free sedimentary gases that was left over after intense degassing of the sediments in the preceding year (Ostrovsky 2009). An increase in pressure stopped gas emission from the compressed sedimentary gas reservoirs in 2003. Thus, the amount of gases in sediments was probably the most important factor affecting some parameters of the echo signal from the bottom in deep areas. These data also indicate that seasonal and inter-annual variations of sedimentary parameters can be large, and can be evaluated with hydroacoustic technology.

The incoherent changes in echo parameters in different parts of the lake (e.g., deep versus shallower areas) in response to water level changes explain why the formal approaches to sediment classifications may be space- and time-specific (Fig. 8). This means that acoustic characterization of bottom sediments should be done cautiously in aquatic systems with varying water level.

Different characteristics of sediments (e.g., compactness, water content, particle size composition, layering, amount of gas bubbles) may be specified and possibly quantified using some echo parameters or their combinations. The complexity in acoustical data interpretation is associated with the complex response of measured parameters, which may be ultimately correlated with each other in one case, but not in another. For instance, surface sediment characteristics (e.g., particle size distribution, porosity, OMC, and algal pigment composition) may strongly correlate with each other along an offshore transect, where a gradient of near-bottom hydrodynamic parameters (turbulence, currents, shear stress) controls resuspension, redistribution, and sorting of various particles (Ostrovsky and Yacobi 1999). On the other hand, in areas adjacent to a river outlet, the composition of bottom sediments may depend on characteristics of the suspended sediment load, particle deposition pattern, and relative amount of autochthonous material. As a result, the relationships between various sediment parameters and their acoustic proxies across a zone like a river outlet may be totally different from those found along other offshore transects. Also, the amount of gases in sediments may correlate with the proportion of fresh organic material, while this relationship may be masked by fluctuations of water level, or changes in intensity of methanogenesis (Ostrovsky 2003). Therefore, future studies should be focused on studying the “purified” impact of specific sedimentary parameters on the echo fingerprint, and then studying and modeling the more complex simultaneous effects of two or more factors. This will allow increase in precision of sediment properties determination using acoustical remote scanning of the bottom.

Acknowledgements We thank L. Lapidus and Y. Kipnis for their assistance with data collection, and J. Harff and Y. Yacobi for their practical comments during preparation of this manuscript. This study was supported by grants from the Israel Science Foundation (211/02, 1011/05), and the German-Israeli Foundation for Research and Development (No. I-711-83.8/2001).

References

- Anderson JT, Holliday DV, Kloser R, Reid DG, Simard Y (2007) Acoustic seabed classification of marine physical and biological landscapes. *ICES Coop Res Rep* 286:1–183
- Anderson JT, Holliday DV, Kloser R, Reid DG, Simard Y (2008) Acoustic seabed classification: current practice and future directions. *ICES J Mar Sci* 65:1004–1011
- Atallah L, Smith PJ, Bates CR (2002) Wavelet analysis of bathymetric sidescan sonar data for the classification of seafloor sediments in Hopvågen Bay—Norway. *Mar Geophys Res* 23:431–442
- Bezdeck JC, Ehrlich R, Full W (1984) FCM: Fuzzy CMeans algorithm. *Comp Geosci* 10(2/3):191–203
- Bowles FA (1997) Observations on attenuation and shear-wave velocity in fine-grained, marine sediments. *J Acoust Soc Am* 101:3385–3397
- Buchanan JB, Kain JM (1971) Measurement of the physical and chemical environment. In: Holme NA, McIntyre AD (eds) *Methods for the study of marine benthos*. Blackwell, Oxford, pp 30–58
- Caughey DA, Kirilin RL (1996) Blind deconvolution of echosounder envelopes. *Proc IEEE Int Conf Acoustics, Speech and Signal Processing ICASSP* 6:3149–3152
- Clough RW, Penzien J (1975) *Dynamics of structures*. McGraw-Hill, New York
- Dubowski Y, Erez J, Stiller M (2003) Isotopic paleolimnology of Lake Kinneret. *Limnol Oceanogr* 48:68–78
- Godet L, Fournier J, Toupoint N, Retière R, Olivier F (2009) Mapping and monitoring intertidal benthic habitats: a review of techniques and a proposal of a new visual methodology for the European coasts. *Prog Phys Geogr* 33:378–402
- Hamilton EL (1972) Compressional-wave attenuation in marine sediments. *Geophysics* 37:620–645
- Hamilton LJ, Mulhearn PJ, Poeckert R (1999) A comparison of RoxAnn and QTCView acoustic bottom classification system performance for the Cairns area, Great Barrier Reef, Australia. *Cont Shelf Res* 19(12):1577–1597
- Holliday DV, Greenlaw CF, Rines JEB, Thistle D (2004) Diel variations in acoustical scattering from a sandy seabed. In: *Proc ICES Conf, 22–25 September 2004, Vigo, 2004/T01 (CD)*. <http://www.ices.dk/products/CMdocs/2004/T/T0104.pdf>
- Ishimaru A (1978) *Wave propagation and scattering in random media*. Academic, New York
- Jickells TD (1998) Nutrient biogeochemistry of the coastal zone. *Science* 281:217–222
- Kohonen T (1987) Adaptive, associative, and self-organizing functions in neural computing. *Appl Optics* 26(23):4910–4918
- Mandelbrot BB (1982) *The fractal geometry of nature*. Freeman & Co, San Francisco
- Mann KH (2000) *Ecology of coastal waters: with implications for management*. Wiley-Blackwell, New York
- Meyers PA, Teranes JL (2001) Sediment organic matter. In: Last WM, Smol JP (eds) *Tracking environmental changes using lake sediments, vol. 2. Physical and chemical techniques*. Kluwer, Dordrecht, pp 239–269
- Middelburg JJ, Levin LA (2009) Coastal hypoxia and sediment biogeochemistry. *Biogeosciences* 6:1273–1293
- Mortensen PB, Dolan M, Buhl-Mortensen L (2009) Prediction of benthic biotopes on a Norwegian offshore bank using a combination of multivariate analysis and GIS classification. *ICES J Mar Sci* 66:2026–2032
- Oliver MA, Webster R (1990) Kriging: a method of interpolation for geographical information system. *Int J Geogr Inf Syst* 4:313–332
- Ostrovsky I (2000) The upper-most layer of bottom sediments: sampling and artifacts. *Arch Hydrobiol* 55:243–255
- Ostrovsky I (2003) Methane bubbles in Lake Kinneret: quantification and temporal and spatial heterogeneity. *Limnol Oceanogr* 48:1030–1036
- Ostrovsky I (2009) The acoustic quantification of fish in the presence of methane bubbles in the stratified Lake Kinneret, Israel. *ICES J Mar Sci* 66:1043–1047
- Ostrovsky I, Yacobi YZ (1999) Organic matter and pigments in surface sediments: possible mechanisms of their horizontal distributions in a stratified lake. *Can J Fish Aquat Sci* 56:1001–1010

- Ostrovsky I, Walline P (2001) Multiannual changes in the pelagic fish *Acanthobrama terraesanctae* in Lake Kinneret (Israel) in relation to food sources. *Verh Int Verein Limnol* 27:2097–2094
- Ostrovsky I, Gophen M, Kalikhman I (1993) Distribution, growth, production and ecological significance of the clam *Unio terminalis* in Lake Kinneret, Israel. *Hydrobiologia* 271:49–63
- Ostrovsky I, McGinnis DF, Lapidus L, Eckert W (2008) Quantifying gas ebullition with echosounder: the role of methane transport by bubbles in a medium-sized lake. *Limnol Oceanogr Methods* 6:105–118
- Pace NG, Ceen RV (1982) Seabed classification using the backscattering of normally incident broadband acoustic pulses. *Hydrogr J* 26:9–16
- Pouliquen E (2004) Depth dependence correction for normal incidence echosounding. In: *Proc 7th European Conf Underwater Acoustics*, ECUA 2004, Delft, The Netherlands, paper 176 (CD)
- Robb GBN, Leighton TG, Dix JK, Best AI, Humphrey VH, White PR (2006) Measuring bubble populations in gassy marine sediments: a review. In: *Proc Institute of Acoustics Spring Conf 2006 Futures in Acoustics: Today's Research—Tomorrow's Careers*, 3–4 April 2006, Southampton, UK, pp 60–68
- Serruya C, Edelstein M, Pollinger U, Serruya S (1974) Lake Kinneret sediments: nutrient composition of the pore water and mud water exchanges. *Limnol Oceanogr* 19:489–508
- Simonsen I, Hansen A, Nes OM (1998) Determination of the Hurst exponent by use of wavelet transforms. *Phys Rev E* 58(3):2779–2787
- Singer A, Gal M, Banin A (1972) Clay minerals in recent sediments of Lake Kinneret (Tiberias), Israel. *Sed Geol* 8:289–308
- Sternlicht DD, de Moustier CP (2003) Time-dependent seafloor acoustic backscatter (10–100 kHz). *J Acoust Soc Am* 114(5):2709–2725
- Tęgowski J (2005) Acoustical classification of the bottom sediments in the Southern Baltic Sea. *Quat Int* 130:153–161
- Tęgowski J (2006) Acoustical classification of bottom sediments (in Polish). *Dissertations and Monographs IO PAS, Sopot*
- Tęgowski J, Lubniewski Z (2002) Seabed characterization using spectral moments of the echo signal. *Acta Acoustica* 88:623–626
- Tęgowski J, Gorska N, Klusek Z (2003) Statistical analysis of acoustic echoes from underwater meadows in the eutrophic Puck Bay (southern Baltic Sea). *Aquat Living Resources* 16:215–221
- Tęgowski J, Klusek Z, Jakacki J (2006) Nonlinear acoustical methods in the detection of gassy sediments. In: *Caiti A, Chapman NR, Hermand J-P, Jesus SM (eds) Acoustic sensing techniques for the shallow water environment. Inversion methods and experiments*. Springer, Berlin, pp 125–136
- van Walree PA, Tęgowski J, Laban C, Simons DG (2005) Acoustic seafloor discrimination with echo shape parameters: a comparison with the ground truth. *Cont Shelf Res* 25:2273–2293
- von Szalay PG, McConnaughey RA (2002) The effect of slope and vessel speed on the performance of a single beam acoustic seabed classification system. *Fisheries Res* 56:99–112
- Wienberg C, Bartholomä A (2005) Acoustic seabed classification in a coastal environment (outer Weser Estuary, German Bight)—a new approach to monitor dredging and dredge spoil disposal. *Cont Shelf Res* 25:1143–1156
- Wilkins RH, Richardson MD (1998) The influence of gas bubbles on sediment acoustic properties: *in situ*, laboratory, and theoretical results from Eckernförde Bay, Baltic sea. *Cont Shelf Res* 18:1859–1892